Differential Precipitation of the Low Energetic Protons and Electrons in Brazilian Anomaly

Sci. Rep. Tôhoku Univ., Ser. 5, Geophysics, Vol. 23, No. 1, pp. 29–36, 1975.

Differential Precipitation of the Low Energetic Protons and Electrons in Brazilian Anomaly

Hiroshi OYA, Akira MORIOKA and Minoru KONDO

Upper Atmosphere and Space Research Laboratory Tohoku University, Katahira, Sendai 980, JAPAN

(Received August 9, 1975)

Abstract: The capacity of a spherical probe immersed in the ionospheric plasma is measured by a radio frequency impedance measuring instrument, that is called gyro-plasma probe, installed on TAIYO (the satellite launched on Feb. 24, 1975). The measured capacity reveals a rapid variation in the regions of the South Atlantic anomaly. This rapid variation is attributed to the soft energetic particle precipitation, that is characterized by the evidence that the flux of a component in the precipitation exceeds the flux of the other species, i.e., the ion flux exceeds the electron flux, vice versa.

1. Introduction

A swept frequency impedance probe called gyroplasma probe (Oya, 1969) has been installed on TAIYO-satellite that was launched on February 24, 1975 into a near earth orbit with low inclination (30°) and with initial perigee and apogee altitudes of 256 km and 3160 km, respectively.

Observations of the electron density and temperature in the full range of the satellite flight path provide a new result associated with the precipitation effect of the energetic particles on the impedance value at 400 kHz. This may reveal a significant modulation of the topside region plasma due to the results of interactions between the high energetic particles and the plasma.

2. A Summary on Theory

A spherical probe with radius 6 cm is used as a RF radio frequency probe. The typical RF characteristics of equivalent capacity for this probe immersed in the space plasma is given in Fig. 1. Due to restricted transmission speed of the telemetry data (64 bits/sec), however, the data handling of impedance measurement is made being sampled automatically by an on-board satellite system. The upper hybrid resonance frequency is measured by detecting the resonance point (see Fig. 1) automatically. After filtering process to minimize high frequency interference, the minimum value at the UHR resonance on the equivalent capacity is obtained by applying differential operation on the measured impedance value. The upper hybrid resonance frequency f_{UHR} gives the electron density N_e, using the electron cyclotron frequency f_c obtained by calculating the magnetic field intensity, as

$$f_p^2 = f_{UHR}^2 - f_c^2 , \tag{1}$$

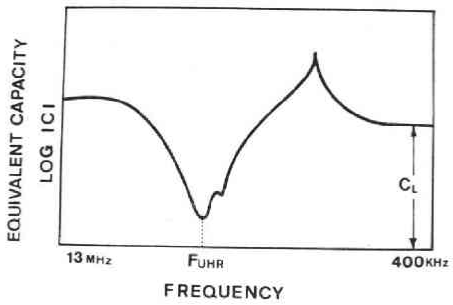

Fig. 1. Schematic illustration of the equivalent capacity plotted versus the swept frequency; F_{UHR} indicates the upper hybrid frequency and C_L is the capacitance value measured at the frequency 400kHz.

and

$$N_e = \left(\frac{m\varepsilon_0 4\pi^2}{e^2}\right) f_p^2 . \tag{2}$$

An impedance value is measured, by giving a sampling signal that is generated when the swept frequency coincides with 400 kHz, to measure an equivalent capacity C_L (see Fig. 1). The capacity C_L at this low frequency gives the ion sheath thickness surrounding the probe since the plasma impedance takes very low values due to free movements of the electron corresponding to RF electric fields. The thickness can be treated in two cases; the first is the case in the ionospheric level and the second is the case in the topside ionosphere or in the plasmasphere. In the ionospheric levels the sheath thickness l is comparable to the Debye's shielding length λ_D; that is, for

$$l = \left(\frac{6}{C_m - 6}\right) R , \tag{3}$$

where R is the probe radius, λ_D is given by

$$\lambda_D = l/\xi . \tag{4}$$

The value ξ can be chosen in a range $2.5 < \xi < 3.0$, assuming that the sheath edge is located at the point where the potential ψ_{edge} is in a range, $0.09 \leq \psi_{edge} \leq 0.14$.

In the region higher than 1000 km, the precipitating particles control the probe potential in a certain area surrounding the South Atlantic anomaly. In this case, it is suitable to assume a thick and homogeneous ion sheath model where no electron can exist in the sheath region due to accumulation of negative charge at the probe. The sheath thickness l surrounding the spherical probe with radius R is obtained from the equation

$$\psi = -\frac{kT}{e}\left(\frac{R}{\lambda_D}\right)^2 \left\{\frac{x^2(2x^2+5x+3)}{6(1+x)}\right\} , \tag{5}$$

using x that is defined by $x = l/R$, where e, k, and T are electron charge unit, Boltsmann constant, and electron temperature, respectively. The x value is again given by

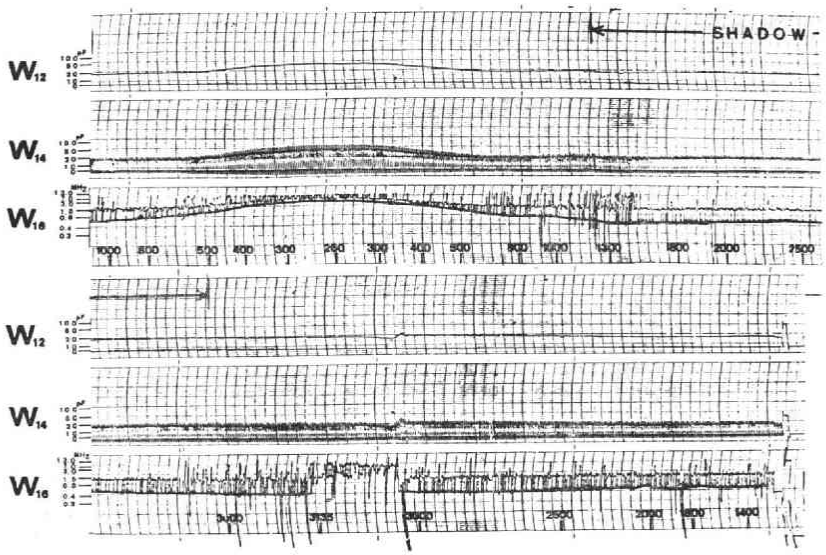

Fig. 2. An example of the quick look data of the gyro-plasma probe measurements obtained for the revolution 22. W_{12} and W_{14} are for C_L measurements, and W_{16} is for the F_{UHR} frequency; the abscissa of the diagram is scaled by the observed height in km. The ecliptic period of the satellite is indicated by "SHADOW".

$$x = \frac{6}{C_m - 6} \ . \tag{6}$$

3. Observation

In Fig. 2, an example of the observation data is given for the revolution number 22 of the satellite path that was carried out from 0808 to 1013 JST on February 28, 1975. In this data W_{12} and W_{14} indicate measured C_L value; in W_{14}, the information is superposed to indicate cut-off frequencies of the filter for the detection of UHR.

The UHR frequency is indicated in the channel given by W_{16} with a thick line, a thin line written as an envelope of sampling signal, in this channel, corresponds to the nf_e resonance, where f_e is the electron cyclotron frequency, with n=3 or 4. The cyclotron harmonic frequency is measured at the high cut-off frequency (150 Hz) of the filter at the differential circuit and the UHR resonance is measured by the low cut-off frequency (40 Hz) of the circuit. These cyclotron harmonic resonances are detected due to the exitation of the electrostatic plasma waves.

The results indicate the profile of the electron density as has been given in Fig. 3. In the bottom panel (see Fig. 3), C_L value has been plotted versus the revolution path. In the ionospheric level this C_L value indicates the temperature as has been given in Table 1. Above the topside ionosphere a peculair variation of the sheath capacitance is revealed as indicated by arrowed interval (see the bottom panel of Fig. 3).

The electron temperature is obtained by using the measured C_L value for these regions of the peculiar variation; the calculated electron temperature T reveals the

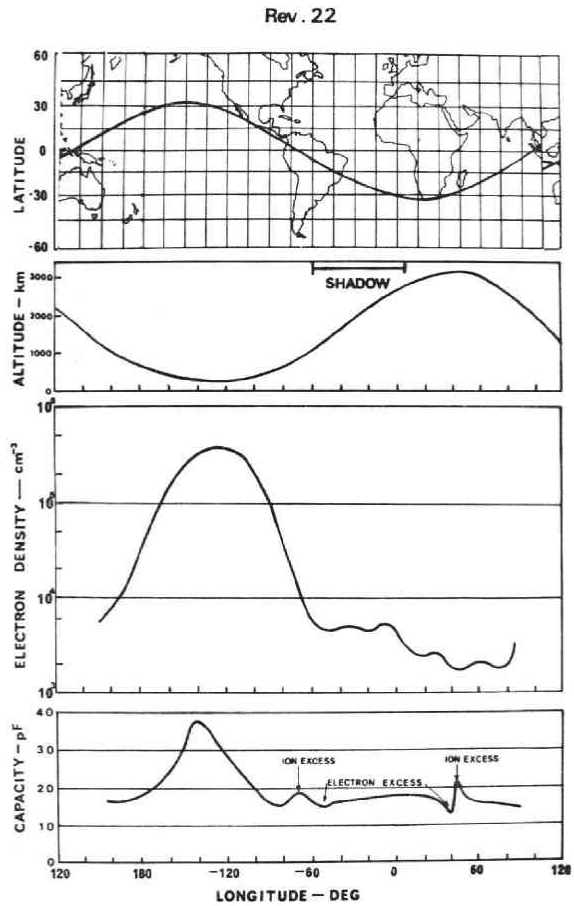

Fig. 3. Calculated electron density and the measured capacity C_L for the revolution 22.

Table 1 Ionospheric Temperature; two values correspond to the models for $\xi=2.8$ and $\xi=3.0$.

Height (km)	$\xi=2.8$	$\xi=3.0$
	°K	°K
250	2060	1800
300	2360	2000
350	2530	2160
400	2660	2280
450	2760	2380
500	2860	2460
550	2930	2540
600	3000	2600

value as $T\simeq 3T_{\text{mean}}$, where T_{mean} is the average value, at the first minimum of C_L near at the region around the longitude –80° (see Fig. 3) and $T\simeq(1/3)T_{\text{mean}}$ at the maximum of C_L value following the first minimum. The same tendency can be obtained near the region around the longitude from –50° to –60°, i.e., $T=0.34T_{\text{mean}}$ at the C_L maximum

and $T=20T_{\text{mean}}$ at the C_L minimum. These rapid variations of the temperature value, in narrow area, is impossible to make interpretation without the energy input to these special regions. We assumed, therefore, precipitation of the energetic particles, i.e., the charging effects on the spherical probe due to the precipitation of particles make the control on the sheath thickness that is produced around the probe. When the energetic electron attacks the probe, the probe absorbs the negative charge and makes a large negative-excursion of the potential; this effect makes the ion sheath thicker than the thickness of the ion sheath without the energetic electron precipitation. When the energetic proton attacks the probe, on the contrary, the positive charge is accumulated on the probe surface, this makes the C_L value larger than the average state.

The calculation of the probe potential with respect to the plasma is made using, for this case, eq. 5. The results indicate the existence of regions where the ion flux exceeds the electron flux, and on the contrary the electron flux exceeds the ion flux of the precipitating particles. This excess precipitation flux is associated with energetic particle precipitation relating to the Brazilian magnetic field anomaly, as will be discussed in following section.

4. Relation with Brazilian Anomaly

Another example of the differential precipitation, where the total proton flux exceeds the electron flux or the electron flux exceeds the proton flux, is given in Fig. 4 for the data obtained in the revolution 48. Since the height is similar for the inbound and outbound edges of the magnetic field anomaly, there is a typical symmetric shape of the differential precipitation that repeats as we can see a "proton flux excess region"

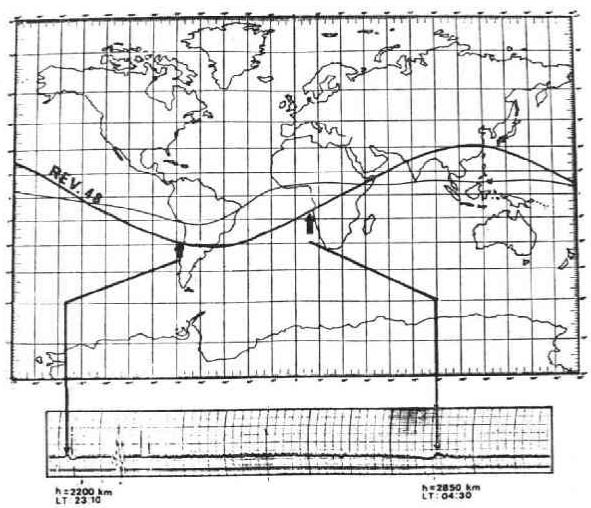

Fig. 4. An example of the differential precipitations observed by the revolution 48; the position of rapid variations of C_L value are observed nearly symmetrically with respect to the center of the South Atlantic anomaly.

before an "electron flux excess region" at the outbound edge, and we can seen an "electron flux excess region" before the "proton flux excess region" at the inbound.

The term ion flux excess is here used, when

$$N_iV_i > N_eV_e\,. \tag{7}$$

The electron excess flux is defined, here, as

$$N_eV_e > N_iV_i\,. \tag{8}$$

where N_i, N_e, V_i and V_e are the ion density, electron density, ion mean velocity and electron mean velocity of the precipitating particles, respectively.

The definitions are made from the following arguments. That is, these fluxes are relating to the probe potential ψ obtained from eq (5) as

$$N_i(V_i+V_{ith}) = N_eV_e+N_e\int_{\sqrt{\frac{2e\psi}{m_e}}}^{\infty} f(\vec{v})\,d\vec{v} \tag{9}$$

where V_{ith} and m_e are the ion thermal velocity and the electron mass; and $f(\vec{v})$ is the electron velocity distribution function in the thermal level. The condition, $N_iV_i > N_eV_e$ gives therefore the decreasing state of ψ while the condition $N_iV_i < N_eV_e$ gives the stage of increasing ψ being compared with the condition $N_iV_i = N_eV_e$.

The variation from the "ion flux excess region" to "electron flux excess region" or variation from "electron flux excess region" to "ion flux excess region" is here called differential precipitation.

These differential precipitations have been observed in all the observation path. All the cases of the observed differential precipitations have been plotted, in Fig. 5, with the calculated precipitation contours for electrons and ions as a reference. It can easily be realized that all the differential precipitations are observed in the regions of the particle flux enhancement due to the Brazilian anomaly of the magnetic field.

5. Discussion

The observation of the VLF hiss has been made near the magnetic equator; the reported positions of this VLF hiss (Gurnet, 1968) coincides with the South Atlantic anomaly. Heikkila (1971) observed particle precipitations in a soft energetic range (50eV$\sim$1keV). The plasma effect was also observed in terms of the local enhancement of the electron density in F2-layer (Knudsen, 1968). Although, no systematic observation has not yet been made for these evidences, all these effect can be identified here, as a result relating to the differential precipitations.

The differential precipitation may suggest that there is an unbalance state of the particle densities between the electrons and ions, in the precipitating regions. This unbalance state may produce a local electric field $\vec{E}$. This local electric field can produces a large variety of reactions such as i) enhancement of the particle precipitations due to $\vec{E}\times\vec{B}$ drifts; and ii) plasma heating due to the generation of electrostatic waves as a result of the drift instabilities.

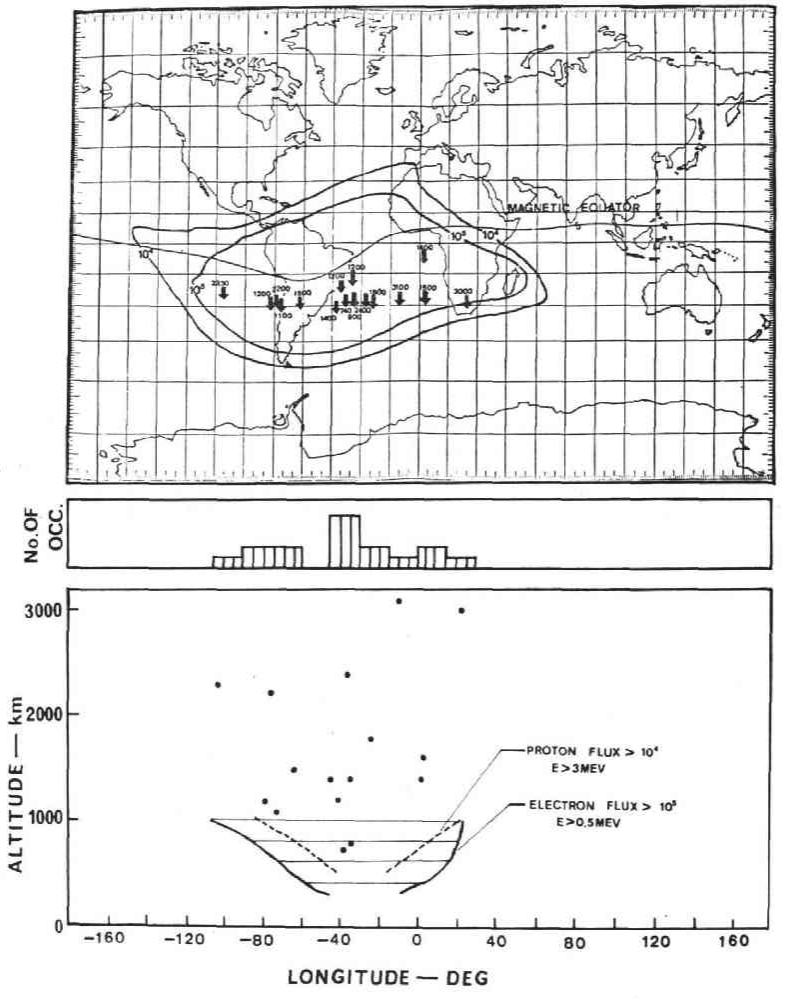

Fig. 5. Mapping (the top panel), the histogram (the middle panel) and the height (the bottom panel) for all of the observed differential precipitations; all the cases are localized within the South Atlantic anomaly. As references, calculated contours for the proton precipitation ($E>3$MeV and with the flux larger than $10^4/cm^2$ sec) and for the electron precipitation ($E > 0.5$ MeV with the flux larger than $10^5/cm^2$ sec) are plotted simultaneously.

6. Conclusion

Successful observations of the impedance measurement by TAIYO give a series of peculiar potential changes of the probe in the region of South Atlantic anomaly. This potential change is interpreted in terms of the soft energetic particle precipitations. The soft energetic particle precipitation is characterized by the unbalance state between the electron flux and the ion flux. Two cases are observed alternatively, i,e., the ion flux exceeds the electron flux at the first region and after passing through this region, the second region, where the electron flux exceeds the ion flux, is followed. The other is the case where the electron flux excess region is observed before the region where the

ion flux excess can be observed. These two cases are called here "differential precipitations".

The differential precipitation is associated with the unbalanced distribution of the ions and electrons. These unbalanced distribution of the charged particles makes a local electric fields that are thought as the main cause of enhanced particle precipitation and the plasma wave instabilities. A series of complex phenomena relating the differential precipitation can be expected; and these remain as new and important subjects for future works.

References

Gurnett, D.A., 1968: Observation of VLF hiss at very low L values, J. Geophys. Res., **73**, 1096.

Heikkila, W.J., 1971: Soft particle fluxes near the equator, J. Geophys. Res., **76**, 1076.

Knudsen, W.C. and G.W. Sharp, 1968: F_2-region electron concentration enhancements from inner radiation belt particles, J. Geophys. Res., **73**, 6275.

Oya, H., 1969: Development of gyro-plasma probe, Small Rocket Instrumentation Techniques — North-Holland Publ. Comp., Amsterdam.